

Article

Genome-Wide Identification and Expression Profiles of IMB Genes Reveal Their Potential Roles in the Gametophytic Sexual Reproduction Process of *Camellia sinensis*

Xiaohan Xu , Anqi Xing, Zichen Wu, Yi Sun, Xuefeng Xu, Shujing Liu , Zhen Zhao, Xuan Chen , Xinghui Li and Yuhua Wang *

College of Horticulture, Nanjing Agricultural University, Nanjing 210095, China; 2019204041@njau.edu.cn (X.X.); 2020204039@stu.njau.edu.cn (A.X.); 2021204039@stu.njau.edu.cn (Z.W.); 2019104085@stu.njau.edu.cn (Y.S.); 2023204057@stu.njau.edu.cn (X.X.); liushujing@njau.edu.cn (S.L.); zhaozhen@njau.edu.cn (Z.Z.); chenxuan@njau.edu.cn (X.C.); lxh@njau.edu.cn (X.L.)

* Correspondence: wangyuhua@njau.edu.cn; Tel.: +86-133-7609-2013

Abstract: It is of great significance to explore the molecular mechanism of gametophytic sexual reproduction in the genetic improvement and breeding of tea plants [*Camellia sinensis* (L.) O. Kuntze]. Imported beta family members (IMBs) are a class of widely distributed nucleoplasmic transport receptor proteins in eukaryotes, affecting plant development and reproduction, and participating in flowering time and sexual reproduction. Still missing, though, is a thorough examination of IMB members in tea plants. Here, seven members of the IMB gene family were screened by a genome-wide investigation in tea plants. These members were scattered unevenly throughout five chromosomes. All of them contained the conserved KAP95 and HEAT Repeat domains. Additionally, the promoter regions of CsIMBs harbored cis-acting elements associated with plant hormones, light, and abiotic stress responses. In order to further confirm the function of CsIMBs in the sexual reproduction of tea plants, the expression patterns of CsIMBs in different flower development stages and the ovary (before and after pollination) were analyzed. The expression results highlighted that CsIMBs were related to the fertility and fruiting of tea plants. Furthermore, five of the seven CsIMBs (CsIMB1a, CsIMB1b, CsIMB2, CsIMB3a, and CsIMB3b) were found to be localized in the nucleus revealed by subcellular localization analysis. These results offer a comprehensive characterization of IMB genes as well as insights into the potential roles of CsIMBs participating in the gametophytic sexual reproduction of *C. sinensis*.

Keywords: *Camellia sinensis*; importin beta protein; expression analysis; gametogenesis



Citation: Xu, X.; Xing, A.; Wu, Z.; Sun, Y.; Xu, X.; Liu, S.; Zhao, Z.; Chen, X.; Li, X.; Wang, Y. Genome-Wide Identification and Expression Profiles of IMB Genes Reveal Their Potential Roles in the Gametophytic Sexual Reproduction Process of *Camellia sinensis*. *Agronomy* **2024**, *14*, 1073. <https://doi.org/10.3390/agronomy14051073>

Academic Editor: Andreas Katsiotis

Received: 23 April 2024

Revised: 15 May 2024

Accepted: 17 May 2024

Published: 19 May 2024



Copyright: © 2024 by the authors. Licensee MDPI, Basel, Switzerland. This article is an open access article distributed under the terms and conditions of the Creative Commons Attribution (CC BY) license (<https://creativecommons.org/licenses/by/4.0/>).

1. Introduction

Tea plant [*Camellia sinensis* (L.) O. Kuntze], as a significant leaf economic crop, contains a lot of theanine, flavonoids, and other health-promoting compounds [1,2]. Cross breeding using tea plant varieties high in polyphenols and amino acids is the key to breeding new and superior varieties. However, tea plants have been subjected to great limitations in conducting hybrid breeding due to the lack of self-incompatibility and low cross-fruiting rate, resulting in a large amount of pollination work often ending up with only a small amount of seeds, leading to the low efficiency of tea plant hybrid breeding and the development of tea plant breeding and genetics research. Therefore, it is of great significance to explore the molecular mechanism of sexual reproduction in tea plants.

Imported beta family (IMB), as a karyopherin (KAP) family, is a kind of nuclear transport receptor protein widely distributed in eukaryotes, which is mainly responsible for the nucleoplasmic shuttle of cytoplasmic protein and participates in flowering time and sexual reproduction [3]. There are two main types of Importin β transport processes. The first type of nucleoplasmic transport relies on junctional proteins, which mediate the nucleoplasmic

transport of substrate molecules containing classical NLS sequences with the assistance of importin α junctional proteins. In this type of transport, the C-terminus of the junction protein importin α has an NLS-binding site that binds to the substrate's entry sequence. The N-terminus has an IBB-binding domain that binds to IMB and stabilizes the importin α -NLS polymer, thus forming a ternary complex for the nucleoplasmic transport of the substrate [4]. Another type of nucleoplasmic translocation does not depend on junctional proteins, and some members of the importin β family are able to directly recognize the entry sequence of substrate molecules and bind to them to mediate the nucleoplasmic translocation of proteins [5]. Gametophyte development is an important prerequisite for plant sexual reproduction. Many proteins that regulate plant gametophyte development depend on the function of IMBs' nucleoplasmic shuttle of cytoplasmic protein to some extent, such as the mitochondrial 50S ribosomal subunit L21, which is encoded by a crucial gene for polar nucleus fusion during female gametophyte maturation and male and female gametophyte recognition during double fertilization, *RPL21M* [6]. Other examples include the ribosomal protein L20 encoded by *GCD1*, which is crucial for polar nucleus fusion and maturation, embryogenesis commencement, and endosperm development [7], and mitochondrial ribosomal protein RPS9M, which is required for central cell maturation [8]. In *rps9m* mutants, the morphology and differentiation of the central cells of female gametophytes are abnormal, and after fertilization, their embryo initiation and early endosperm development are severely affected [8].

More and more members of the IMB protein family have been identified in the model plant *Arabidopsis thaliana*, and results have been obtained on the functions of related protein members during plant reproductive development. The deletion of *AtIMB3/AtKETCH1* leads to reduced ribosome biogenesis and translation, which may trigger a stalling of mitotic cell cycle progression, resulting in gametophytic lethality [9]. *AtIMB4* can interact with transcriptional co-activators GRF-INTERACTING FACTORS (GIFs) to regulate the growth of the bead cover by mediating the translocation of GIFs into the nucleus, which in turn affects plant development and reproduction processes [10]; *XPO1A* and *XPO1B* are involved in the gametophytic sexual reproduction process [11], and *XPO1A* is also involved in the heat response pathway [12]; *HASTY/XPO4* is involved in the maintenance of stem meristems, flowering time, and sexual reproduction [13,14].

However, so far, there are still gaps in the comprehensive identification and characteristic analysis of the IMB members in *C. sinensis*. In this study, seven IMB proteins were identified from *C. sinensis*. The structural features and phylogenetic relationships of *C. sinensis* importin-beta (*CsIMB*) proteins were analyzed. The expression pattern of the seven *CsIMB* genes in the pollinated ovary of three *C. sinensis* cultivars was investigated to explore their roles in the reproductive development of tea plants.

2. Materials and Methods

2.1. Identification of IMB Family Genes in *C. sinensis*

Using Local BLASTp and Bioedit (v8.1.0, Manchester, UK), the amino acid sequence of the *C. sinensis* genomic coding sequences (<http://tpia.teaplant.org/index.html>) (accessed on 10 October 2023) was compared to the known IMB gene family of *A. thaliana* (<https://www.arabidopsis.org/>) (accessed on 10 October 2023). Additionally, the candidate IMB genes of *C. sinensis* were verified using the Pfam protein analysis online services (<http://pfam.xfam.org/>) (accessed on 10 October 2023) and the SMART online services (<http://smart.embl-heidelberg.de/>) (accessed on 10 October 2023), and ultimately, the members of the *CsIMB* family were identified.

2.2. Phylogenetic Analysis and Structural Characterization

The phylogenetic tree was created using MEGA 11.0, the Neighbor-Joining technique, and relevant settings (Poisson model, pairwise deletion, and 1000 bootstrap replications). ClustalW was utilized to compare the domains of *CsIMBs* and *AtALMTs* [15]. Every detected *CsIMB* was categorized and given a name based on the evolutionary connection

and the AtIMB sequence classification. In this investigation, uniform naming guidelines were implemented. In short, the prefix 'Cs' (*Camellia sinensis*) was used to name each IMB gene sequence, and extra numerals, such *CsIMB1*, *CsIMB2*, and so forth, were used to differentiate them.

Using the ExPASy-ProtParam web services (<https://web.expasy.org/protparam/>) (accessed on 10 October 2023), the fundamental physical and chemical characteristics of the CsIMB protein, such as its average hydrophobicity and amount of amino acids, were predicted. TMHMM Server.2.0 (<http://www.cbs.dtu.dk/services/TMHMM>) (accessed on 10 October 2023) was utilized to perform the subcellular localization analysis of CsIMB proteins.

The *C. sinensis* genome annotation file (http://www.plantkingdomgdb.com/tea_tree/data/gff3/) (accessed on 10 October 2023) and the conserved structure of CsIMBs were used to build the schematic diagram of the *CsIMB* gene structure using the TBtools web tool (<https://github.com/CJ-Chen/TBtools>) (accessed on 10 October 2023). The conserved motif (E-Value < 20) of the CsIMB amino acid sequence was found using the MEME online service (<http://meme-suite.org/tools/meme>) (accessed on 10 October 2023), and the structural map of CsIMBs was created using TBtools.

2.3. Cis-Element Analysis

Promoter sequences were defined as those that were 2000 base pairs upstream of the *CsIMB* gene's transcription start site (ATG). The 2000 bp upstream sequence of *CsIMBs* was extracted by TB Tools Web Tool (<https://github.com/CJ-Chen/TBtools>) (accessed on 10 October 2023) using the *C. sinensis* gff3 file. The PlantCARE database (<http://bioinformatics.psb.ugent.be/webtools/plantcare/html/>) (accessed on 10 October 2023) was utilized to assess potential cis-acting regulatory elements (CREs) based on these promoter sequences.

2.4. Chromosomal Locations of IMB Genes in Tea Plant

The gff files and IDs of the CsIMB were used to map the positions of the CsIMB genes by TBtools program in order to explore the chromosomal locations of the *CsIMB* gene in tea plants [16].

2.5. Plant Materials and Crossbreeding Treatment

In this study, one tea plant variety 'HuangJinYe' with a high natural fruiting rate and two low natural fruiting rate tea plant varieties 'BaiYe1' and 'HuangJinYa' which were grown in the same tea plantation at the Tea Research Institute of Tianmu Lake in Liyang, Changzhou, Jiangsu, China (31°20' N, 119°23' E) were selected as the hybrid parents, and 'Longjing 43' growing in Jiangsu Tea Expo Park, Zhenjiang, Jiangsu, China (31°55' N, 119°15' E) was selected as the hybrid parent. Controlled pollination was carried out in early November during the white bud stage in the following three years (2020–2022). The buds were castrated, bagged, and pollinated the next day between 8:30–11:00 and 13:00–16:30, and re-bagged immediately after pollination. The pistils were collected at 72 h after pollination (HAP), liquid nitrogen-snap-frozen right away, and kept at −80 °C. A total of 300 pollinated pistils were collected (100 each from 'HuangJinYe', 'BaiYe1', and 'HuangJinYa'), and the rest were left in the field for monitoring the fruiting rate.

2.6. RNA Extraction, cDNA Synthesis, and Quantitative Real-Time RT-qPCR

For the expression patterns analysis in different *C. sinensis* tissues, total RNA was extracted from three tissues (leaf, young stem, and mature stem) and three stages of flower development [flower S1 (young bud stage), flower S2 (white bud stage), and flower S3 (full bloom stage)], the division of flower development stages according to Xu et al. [17] for 'Huangjinye', 'Huangjinya', and 'Baiye1' of three independent biological replicates using EASYspin Plus Complex Plant RNA Kit (Aidlab, Beijing, China, Cat No. RN53). For the expression patterns analysis in *C. sinensis* reproduction process, total RNA was extracted from unpollinated and pollinated pistils of three independent biological replicates using

EASYspin Plus Complex Plant RNA Kit (Aidlab, Beijing, China, Cat No. RN53). Total RNA quality was verified using a 2100 Bioanalyzer RNA Nano chip device (Agilent, Santa Clara, CA, USA) and a NanoDrop ND-1000 spectrophotometer (NanoDrop, Wilmington, DE, USA) according to Wang et al. [18]. For RT-qPCR analysis of *CsIMBs*, HiScript[®] III RT SuperMix for qPCR (with gDNA wiper) (Vazyme, Nanjing, China, Cat No. R323-01) and the Oligo(dT)₂₀ VN was used to synthesize the first-strand cDNA. The RT-qPCR analysis was conducted using the ChanQ[®] SYBR qPCR Master Mix (Vazyme, Nanjing, China, Cat No. Q311-02) with the specific primer pairs shown in Table S1. *Csβ-Actin* and *CsGADPH* served as reference genes [15].

The Bio-Rad BFX96 fluorescence (Bio-Rad C1000 Touch[™] Thermal Cycler, Bio-Rad, Hercules, CA, USA) was used for all the RT-qPCR assays. Three technical repeats and three biological repeats were used for each sample. No template control and no reverse-transcriptase control were included as the negative control. At the conclusion of the RT-qPCR test, the melting-curve examination of the amplified products verified the specificity. Using the $2^{-\Delta\Delta C_t}$ technique, the expression levels of *CsIMBs* were standardized to *Csβ-actin* [19]. Table S1 in Supplementary Materials contains a list of all the gene-specific primers.

All the RT-qPCR tests were performed on the Bio-Rad BFX96 fluorescence (Bio-Rad C1000 Touch[™] Thermal Cycler, CA, USA). Each sample was run in three technical triplicates with three biological replicates. The specificity was confirmed by the melting-curve analysis of the amplified products at the end of the RT-qPCR test. The expression levels of *CsIMBs* were normalized to the *Csβ-actin* based on the $2^{-\Delta\Delta C_t}$ method. All the gene-specific primers are listed in Table S1.

2.7. Gene Clone and Subcellular Analysis of *CsIMB*

In order to obtain the complete open reading frame (ORF) of *CsIMBs*, mixed cDNA (from unpollinated and pollinated pistils) and primers with homologous arms were used (Table S1). For subcellular localization, the ORF of *CsIMB1a*, *CsIMB1b*, *CsIMB2*, *CsIMB3a*, and *CsIMB3b* without its stop codon was ligated with a vector to generate pCAMBIA1300-*CsIMB1a*-GFP, pCAMBIA1300-*CsIMB1b*-GFP, pCAMBIA1300-*CsIMB2*-GFP, pCAMBIA1300-*CsIMB3a*-GFP, and pCAMBIA1300-*CsIMB3b*-GFP under the control of the Ubiquitin promoter. The vector pCAMBIA2300-35S-H2B-mCherry was used as a marker vector for nuclear localization. The vectors were then introduced into *Agrobacterium tumefaciens* strain GV3101 by *Agrobacterium*-mediated transformation.

Twenty-day tobacco leaves were infected with the altered *A. tumefaciens* cells [20]. After 3-day incubation in the dark, the GFP fluorescence was detected by an ultra-high-resolution confocal microscope (Zeiss LSM800, Zeiss, Oberkochen, Germany).

2.8. Statistical Analysis

All online services were accessed on 10 October 2023. Data analysis and correlation analysis were performed using the SPSS software (SPSS Inc. version 22.0, Chicago, IL, USA, 2013) under Duncan's test. The data diagrams were drawn with the R software (version 4.3.0).

3. Results

3.1. Identification and Chromosome Location of *IMB* Genes in *C. sinensis*

Based on the existence of conserved KAP95, importin_rep_4, importin_rep_6, and HEAT Repeat domains, a total of seven *IMB* genes were found in the genome of the tea plant (Figure S2). Each *CsIMB* has a preserved structural domain for KAP95, which was highly conserved at the N-terminal of the *CsIMB* proteins. In addition, only *CsIMB3a* and *CsIMB3b* contained importin_rep_4 and importin_rep_6 conserved structural domain. On the other hand, all seven *CsIMB* genes contained multiple HEAT Repeat domains. They were named as *CsIMB1a*, *CsIMB1b*, *CsIMB1c*, *CsIMB1d*, *CsIMB2*, *CsIMB3a*, and *CsIMB3b* according to the phylogenetic relationship (Figure 1A). According to the chromosomal

position, CsIMB1a was identified on chromosome 3, chromosome 9 was found to contain CsIMB1b and CsIMB1c, and CsIMB2 and CsIMB3a were found on chromosome 6 and chromosome 7, respectively. Two (CsIMB1d and CsIMB3b) members were found on chromosome 12 (Figure S1).

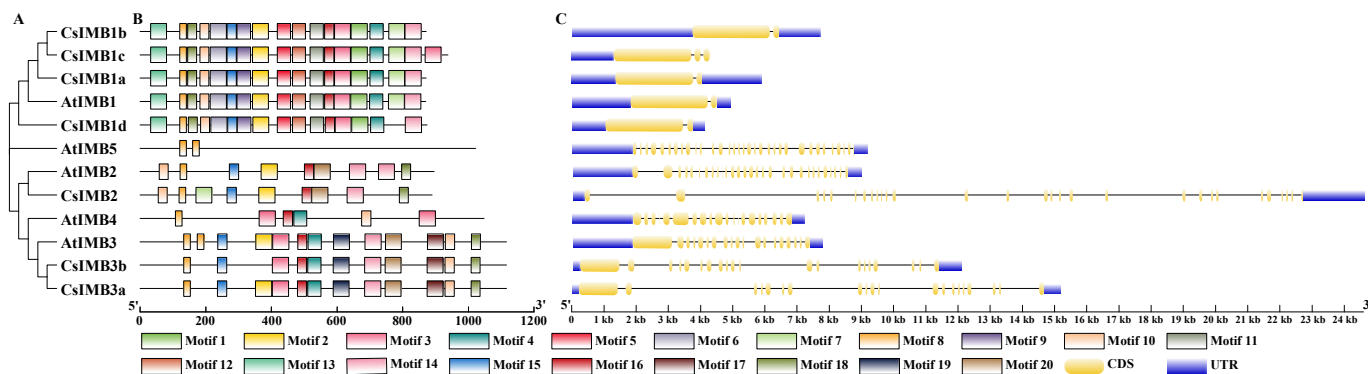


Figure 1. Phylogenetic relationship, the distribution of conserved motifs, and the gene structure of CsIMB proteins in *C. sinensis*. (A) The phylogenetic tree of the CsIMB and AtIMB gene family members. (B) The distribution of the conserved motifs of the proteins encoded by CsIMBs. Different motifs are indicated by different colored numbered boxes. (C) The distribution of UTRs and CDSs of the CsIMB gene family members. Yellow represents CDSs and blue represents UTRs.

The CsIMB genes coded for 871 amino acids (CsIMB1a and CsIMB1b) to 1116 amino acids (CsIMB3a and CsIMB3b). CsIMB1b had a relative molecular weight of 96.41 kDa, while CsIMB3a had a molecular weight of 123.55 kDa (Table 1). CsIMB proteins have an isoelectric point distribution ranging from 4.60 (CsIMB1b) to 4.90 (CsIMB2). For each of the seven CsIMB proteins, the subcellular localization was expected to reside in the nucleus. Notably, only CsIMB1c has an average hydrophilicity greater than zero. As shown in Table S2, the total number of negatively charged residues (Asp + Glu) ranged from 118 (CsIMB1a, CsIMB1c, and CsIMB2) to 159 (CsIMB3b) and the total number of positively charged residues (Arg + Lys) was between 64 (CsIMB1c) and 96 (CsIMB3b). The instability index ranged from 44.54 (CsIMB1b) to 52.24 (CsIMB2) and the aliphatic index was between 97.04 (CsIMB1b) and 101.92 (CsIMB2).

Table 1. CsIMB genes identified in *C. sinensis*.

Gene Name	Gene ID	Number of Amino Acids (aa)	Molecular Weight (Da)	Theoretical pI	GRAVY	Subcellular Localization
CsIMB1a	XM_028230465.1/TEA026073.1	871	96,494.45	4.63	−0.013	Nuclear
CsIMB1b	XM_028243725.1/TEA017020.1	871	96,406.30	4.60	0	Nuclear
CsIMB1c	XM_028243724.1/TEA017025.1	938	103,663.70	4.67	0.022	Nuclear
CsIMB1d	XM_028221219.1/novel_T012380	874	96,554.43	4.76	−0.007	Nuclear
CsIMB2	XM_028242114.1/novel_T023108	889	99,671.85	4.90	−0.011	Nuclear
CsIMB3a	XM_028207439.1/TEA014745.1	1116	123,553.65	4.73	−0.063	Nuclear
CsIMB3b	XM_028214489.1/novel_T007067	1116	123,538.34	4.73	−0.076	Nuclear

The findings of the CsIMB phosphorylation sites by KinasePhos revealed that the number of threonine (T) kinase phosphorylation sites ranged from 13 to 33, serine (S) kinase phosphorylation sites ranged from 41 to 58, and tyrosine (Y) kinase potential phosphorylation site was between 5 and 10 (Table S2 and Figure S3). The anticipated outcomes of the CsIMB's secondary structure showed that the α -helix percentage was between 71.09% and 77.69%, the extended chain percentage was between 0.69% and 4.48%, the β -turn percentage was between 0.57% and 2.42%, and random coil ranged from 18.82% to 23.28%

(Table S2 and Figure S4). Furthermore, the homologous modeling (tertiary structure) revealed a significant degree of structural similarity between CsIMB1a-d and CsIMB3a and CsIMB3b, reaching up to 90% (Figure S5).

3.2. Conserved Motif and Gene Structure Analyses

A total of 20 motifs, dubbed motif 1 through motif 20, were found in CsIMBs and AtIMBs according to the protein conserved motif analysis (Figure 1B), with the majority of the motifs being in the same order (Figure 1B). It is worth noting that the motifs contained in AtIMB1-5 and their order of arrangement varied considerably. However, the motifs of CsIMB1a-d were arranged in a highly similar order to AtIMB1, CsIMB2 is highly similar to AtIMB2, and CsIMB3a-b were highly similar to AtIMB3. Sequence alignment showed that all motifs except motif 7, motif 14, motif 17, and motif 20 corresponded to the KAP95 domain, and motif 7, motif 14, motif 18, and motif 20 corresponded to the importin_rep_6 domain, but only motif 9 corresponded to the importin_rep_4 domain, respectively (Figures 1B and S2). By comparing the cDNA sequences of CsIMBs with matching genomic sequences, we were able to analyze the exon–intron structures and thereby define the structural variety of the IMB genes (Figure 1C). The results showed that the gene structures of CsIMB1a, CsIMB1b, and CsIMB1d were very similar to those of AtIMB1, and they all had only two exons. CsIMB1c had three exons, but it was worth noting that it did not have a 3' UTR region. In addition, both CsIMB2 and AtIMB2 had 29 exons, and their exons were very similar in length and arrangement order. Furthermore, CsIMB3a and CsIMB3b had 20 exons, but AtIMB3 had only 19 exons, which might be due to the different evolutionary ways of homologous genes in different species. However, CsIMB3a, CsIMB3b, and AtIMB3 all had an exon of about 1200 bp after the 5' UTR region.

3.3. Cis-Acting Element Analysis of CsIMB Promoters

Thirty different cis-acting element types were found and categorized into five groups: abiotic stress-responsive, light-responsive, core promoter element, hormone correlation, and cell development-related elements (Figure 2 and Table S3). Among the cis-acting elements found in the CsIMB family members' promoter regions, core promoter elements were the most numerous, followed by light-responsive elements, and developmentally related elements were the least numerous. All CsIMB genes contained core promoter elements. Some cis-elements were specific to certain CsIMB genes such as the 3-AF1 binding site, Gap-box and AuxRR-core (CsIMB1b), AAAC-motif, GA-motif and I-box (CsIMB1a), ACE (CsIMB1d), and AuxRE (CsIMB3a). Nine cis-acting regulatory factors, including methyl jasmonate (MeJA), salicylic acid (SA), gibberellin (GA), auxin, and abscisic acid (ABA), were shown to be associated with hormone responses, but only two kinds of abiotic stress elements were found (LTR, low-temperature responsiveness; MBS, MYB binding site involved in drought-inducibility). In addition, all seven CsIMB genes were found to contain at least one phytohormone-responsive element.

3.4. Tissue-Specific Expression of CsIMB Genes

The expression levels of CsIMBs demonstrated unique expression patterns in several cohorts (Figure 3). Nearly all CsIMBs were expressed in all chosen tissues at different developmental stages, as seen by the heatmap. Among them, the expression levels of CsIMB1a-c gradually increased with flower development and were lower in young stems than in flower S3. In particular, the expression levels of CsIMB1a-c were lower in the mature stems of 'Huangjinya' and 'Baiye1' than in flower S3, whereas the expression levels of CsIMB1a-b were higher in the mature stems of 'Huangjinye' than in flower S3. In addition, the expression levels of CsIMB3a-b increased significantly from flower S1 to flower S2, and decreased slightly to S3 in 'Huangjinye'. However, in 'Huangjinya' and 'Baiye1', the expression levels of CsIMB3a-b of both flower S1 and flower S2 were lower than that of flower S3. It is noteworthy that only the expression levels of CsIMB3a-b in the leaves, young stems, and mature stems of 'Huangjinya' were lower than that of flower S3, while in

‘Huangjinye’, the expression levels of 3a-b in the leaves and mature stems were higher than that of flower S3. For *CsIMB1d*, the expression level in flower S3 of ‘Huangjinye’ was lower than that in all other tissues, and the expression level in flower S2 of ‘Baiye1’ was lower than that in flower S3, but higher than that in flower S3 in all other tissues. The expression levels of *CsIMB2* were higher in flower S2 and the mature stems of all three cultivars, and lower in flower S3, flower S1, and young stems.

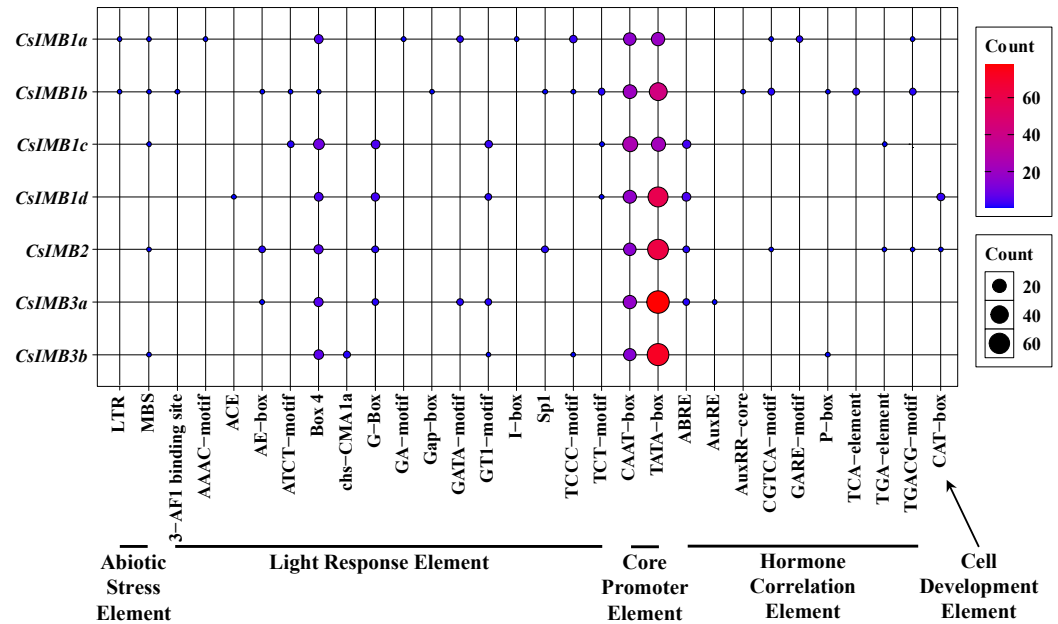


Figure 2. Analysis of the *cis*-acting elements of the 7 *CsIMB* genes. The *cis*-acting elements were classified into 5 types: abiotic stress elements, light response elements, core promoter elements, hormone correlation elements, and cell development elements. The size and color of the solid circle indicate the number of the *cis*-acting elements of *CsIMBs*.

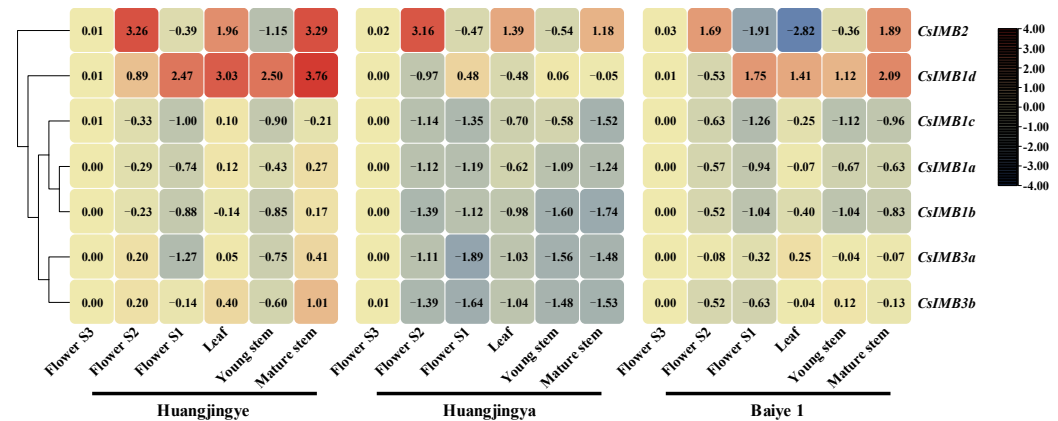


Figure 3. *CsIMB* gene expression patterns in three tissues and three stages of flower development. S1–S3 represent the young bud stage, white bud stage, and full bloom stage of *C. sinensis* flower developmental stages via RT-qPCR. The numbers in the grid are obtained by the logarithmic transformation of the original relative expression level. The red and blue colors represent high and low expression levels, respectively.

3.5. Fruiting Rate and Expression Analysis of *CsIMBs* in Response to Pollination

All seven *CsIMB* genes were found significantly up-regulated after the pollination in ‘Huangjinye’ (Figure 4). The expression levels of *CsIMB1a*, *CsIMB2*, and *CsIMB3a* were down-regulated after the pollination, but the expression levels of *CsIMB1b*, *CsIMB1c*,

CsIMB1d, and *CsIMB3b* had no significant change after the pollination in both ‘Huangjinya’ and ‘Baiye1’. Notably, the expression of *CsIMB1c* and *CsIMB1d* in ‘Baiye1’ increased significantly after pollination, but the expression of *CsIMB3b* decreased significantly. Furthermore, the three-year average hand-pollinated fruiting rate showed that ‘Huangjinya’ far exceeded ‘Huangjinye’ and ‘Baiye1’ (Table 2).

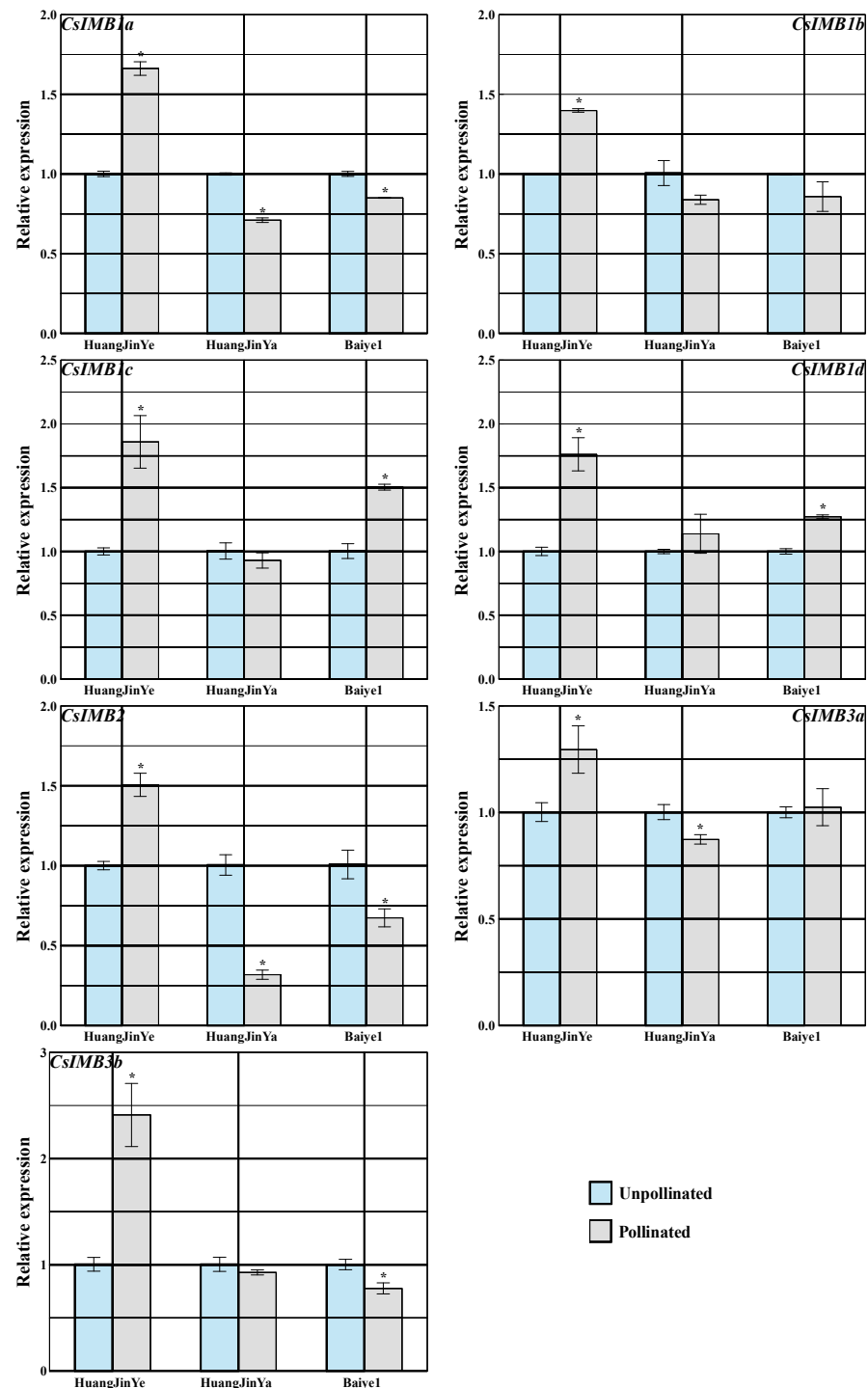


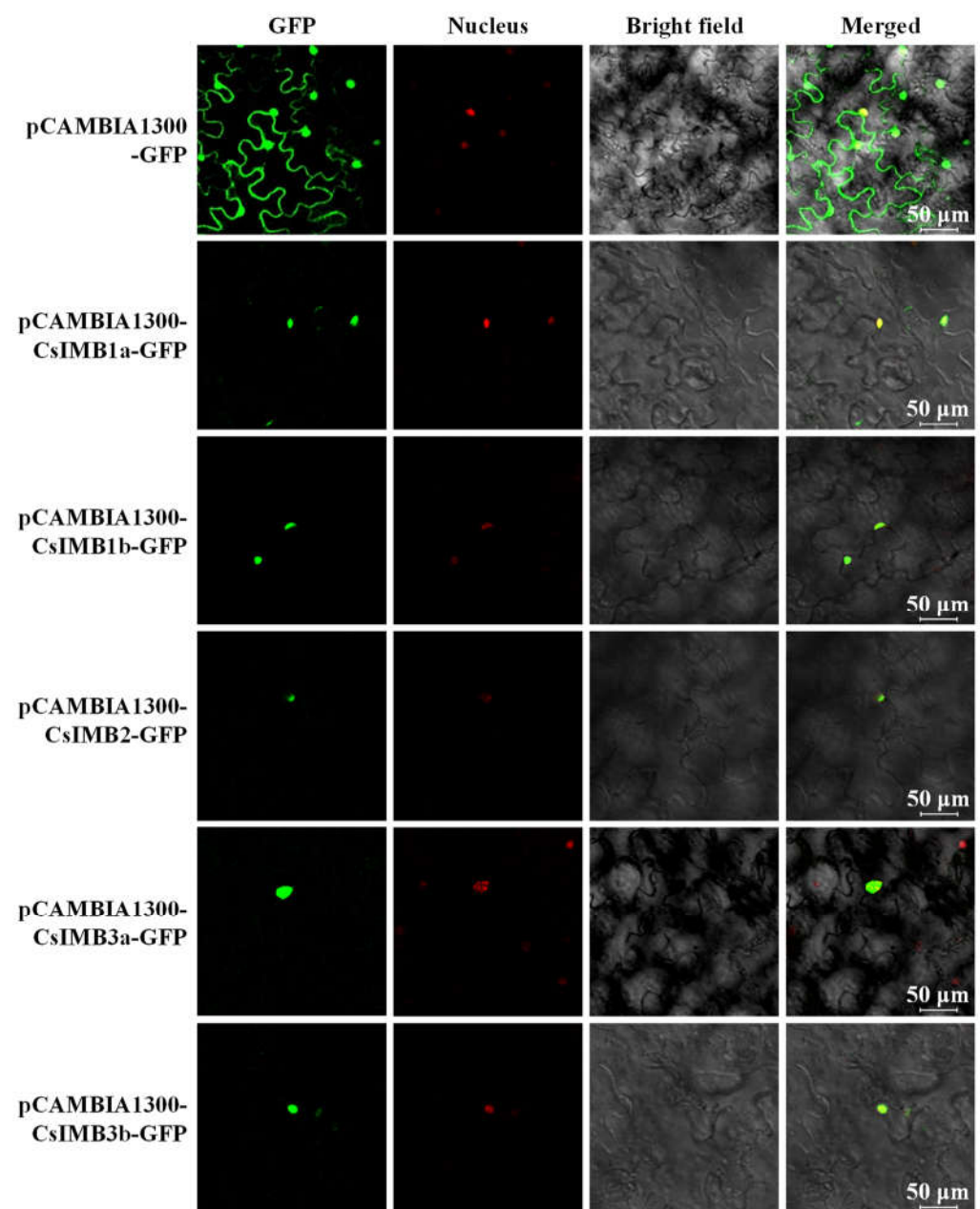
Figure 4. Expression patterns of the *CsIMB* gene in the ovary (each treatment used cDNA synthesized from total RNA extracted from 20 ovaries) before the pollination and 72 h after the pollination via RT-qPCR. * represents that the expression patterns of *CsIMB* have significant differences between the unpollinated and pollinated ovaries in the same tea cultivar ($p < 0.05$), as determined by the Duncan test.

Table 2. Fruiting rate of three *C. sinensis* cultivars.

Cultivar	Seed Rate (%)			Mean
	2020–2021	2021–2022	2022–2023	
Huangjinye	79.55	76.92	65.85	74.11
Huangjinya	28.57	27.91	7.32	21.27
Baiye1	28.00	23.81	20.00	23.94

3.6. Subcellular Analysis of CsIMB

In order to further verify whether CsIMBs participate in the gametophyte sexual reproduction process through nucleoplasmic transfer receptor-mediated protein entry and exit functions, the subcellular localization analyses were used to examine the functions of CsIMB1a, CsIMB1b, CsIMB2, CsIMB3a, and CsIMB3b (Figure 5). The findings supported the hypothesis by showing that these CsIMBs reside in the nucleus (Table 1).

**Figure 5.** Subcellular localization of CsIMB1a, CsIMB1b, CsIMB2, CsIMB3a, and CsIMB3b.

4. Discussion

In eukaryotic cells, gene replication, transcription, and protein expression and translation take place in intracellular compartments, and the transport of biomolecules such as proteins and nucleic acids across the nuclear membrane has become one of the most important biological functions in cells. Generally speaking, molecules with molecular weight less than 50 kDa can pass through the nuclear pore complex (NPC) by free diffusion, while biomolecules with molecular weight greater than 50 kDa can only undergo nucleoplasmic transfer by active transport, which is mainly accomplished by the members of the IMB family of proteins [21]. A thorough examination and synopsis of the shared traits of the members of the tea plant IMB gene family are lacking. In our investigation, seven IMB genes of *Camellia sinensis* containing KAP95, importin_rep_4, importin_rep_6, and HEAT Repeat conserved domains were identified. HEAT is a helical rod-shaped structural unit consisting of the consecutive repeats of 37–46 amino acids. HEAT Repeats consist of multiple such units superimposed to form a ductile superhelix, which can provide abundant binding sites for interacting proteins through conformational changes. With this specialized structure, the members of the importin β family can use the C-terminus to bind substrates (cargos) [22] or adaptor proteins [23], the N-terminus to bind RanGTP [24], and the middle to bind nuclear pore proteins (Nups) [25] to bring substrates into or out of the nucleus. By analyzing the crystal structure of importin β , the HEAT Repeat superhelical structural domains in it can stretch or contract, changing various conformations to match substrates with different structures. Moreover, importin β can use four types of junction proteins to recognize different types of substrates. On the other hand, these seven CsIMB genes are dispersed erratically throughout the five chromosomes of the tea plant, with certain CsIMBs forming unique gene clusters (Figure S1).

The tea plant genome provided the CsIMB gene structural features, as per the genome annotation file (Figure 1 and Table 1). The length of the CsIMB genes varied significantly according to the results. The gene length for each AtIMB and CsIMB was less than 4 kb. Research has shown that the gain/loss of an exon or an intron contributes to the structural and functional variety of genes [26]. Only CsIMB1c does not have the 3'-UTR region according to a thorough examination of the exon-intron structure and sequence length of the CsIMB genes.

The classification and function prediction of the CsIMB gene family are made easier by the discovery of conserved motifs. Only five of the twenty conserved motifs were present in all seven CsIMBs. (Figure 1B). Specifically, no CsIMB contains all 20 conserved motifs, and CsIMB1c has the most conserved motif (18). In the meantime, there was a significant variation in the motifs found in the various members of CsIMB, indicating that genes within different branches might have diverse functions. This is in line with other investigations that have shown the involvement of AtIMB1/AtKPNB1 in the ABA-mediated drought stress response [27], while AtIMB3/AtKETCH1 is critical for the nuclear accumulation of ribosomal proteins and gametogenesis [9].

The essential regulators of protein transcription are found in the cis-acting regions of genes. Cis-acting element analysis showed that phytohormone stimulation signals, such as ABA, auxin, GA, SA, and MeJA, regulated CsIMB members (Figure 2 and Table S3). They may also be transcribed in response to an abiotic stressor, but only the MYB binding site that is responsible for drought-inducibility would do so. Furthermore, all seven CsIMBs were responsive to light.

The expression of the CsIMB gene family in different tissues has been conducted in this study (Figure 3). The CsIMB family has a variety of expression patterns that are used to perform tasks particular to different tissues. The findings demonstrated that the seven CsIMBs could be grouped into four clusters using clustering analysis. Genes in the same cluster had comparable expression patterns, suggesting possible functional redundancy and co-regulation. On the one hand, the expression levels of CsIMB1a-c gradually increased with flower development suggesting that they play a crucial role in flower development and even fertility. Moreover, CsIMB3a-b had similar expression patterns during flower

development with *CsIMB1a-c*. On the other hand, *CsIMB1d* showed a decreasing and then increasing expression pattern during flower development, whereas *CsIMB2* showed an increasing and then decreasing pattern. This suggests that the two genes act at different stages of flower development, i.e., *CsIMB2* is mainly involved in the initial development of tea plant flowers, whereas *CsIMB1d* is more associated with tea plant flowering or fertility. Notably, unlike *CsIMB1a-c* and *CsIMB3a-b*, *CsIMB1d* and *CsIMB2* had higher expression levels in the leaves and mature stems of ‘Huangjinye’, suggesting that *CsIMB1d* and *CsIMB2* are more inclined to function in mature tissues in ‘Huangjinye’. The analysis of the tissue-specific expression pattern of the *CsIMB* gene will provide important insights for further studies on the function of the *CsIMB* gene in tea plants.

Since the *CsIMB* gene may play a crucial role in the development and fertility of tea plants, we analyzed the expression pattern of the *CsIMB* gene and its fruiting rate in three tea plant cultivars before and after artificial pollination. All seven *CsIMBs* showed a significantly up-regulated expression pattern in ‘Huangjinye’ after pollination and were different from both ‘Huangjinya’ and ‘Baiye1’ (Figure 4). On the other hand, ‘Huangjinye’ also showed a higher hand-pollinated fruiting rate than both ‘Huangjinya’ and ‘Baiye1’ (Table 2). These results indicate that these *CsIMBs* are likely to play an important role in the fertility and fruit-bearing of tea plants. This conjecture is consistent with the reported conclusion that *AtIMB3/AtKETCH1* is essential for gametogenesis [9]. Furthermore, the fluorescence of subcellular localization for some members of *CsIMBs* showed that they were located in the nucleus which is consistent with its nucleoplasmic transfer receptor-mediated protein entry and exit functions.

5. Conclusions

This study identified seven *CsIMB* genes in *C. sinensis* and conducted a systematic analysis of their properties, including expression patterns, phylogenetic tree, chromosomal localization, gene structures, and promoter cis-acting elements. The functional characterization was performed through subcellular localization and crossbreeding treatment. The findings demonstrated that *CsIMBs* were unevenly distributed on five chromosomes and could be divided into three groups. The conserved HEAT Repeat structural domain and KAP95 structural domain were present in all *CsIMBs*. The promoters of *CsIMBs* contained elements relevant to cell development, hormone correlation, abiotic stress response, light response, core promoter element, and cis-acting element prediction. The seven members of the *CsIMB* gene family have distinct expression patterns in four distinct tissues and three phases of floral development, as demonstrated by the tissue-specific analysis, indicating their significant roles in plant growth and development. All seven *CsIMBs* may be related to the fertility and fruiting of tea plants. This study provides a potential approach and inspiration for further study of the potential roles of the *CsIMB* gene family in the gametophytic sexual reproduction process.

Supplementary Materials: The following supporting information can be downloaded at: <https://www.mdpi.com/article/10.3390/agronomy14051073/s1>, Figure S1: The chromosomal location of the *CsIMB* genes; Figure S2: Conserved domain of *CsIMB* proteins; Figure S3: Phosphorylation site of *CsIMBs*; Figure S4: Secondary structure of *CsIMBs*; Figure S5 Tertiary structure of *CsIMBs*; Table S1: Primers for PCR; Table S2: Analysis of amino acid sequence characteristics of *CsIMB* gene family in *C. sinensis*; Table S3: Details of the cis-acting elements in the promoter region (−2000 bp) of the *CsIMB* genes.

Author Contributions: Conceptualization, X.X. (Xiaohan Xu) and Y.W.; methodology, X.X. (Xiaohan Xu); validation, X.X. (Xiaohan Xu), Y.W. and Z.Z.; formal analysis, X.X. (Xiaohan Xu); investigation, X.X. (Xiaohan Xu); data curation, X.X. (Xiaohan Xu), A.X., Z.W., Y.S., X.X. (Xuefeng Xu) and Z.Z.; writing—original draft preparation, X.X. (Xiaohan Xu); writing—review and editing, X.X. (Xiaohan Xu), S.L., X.C., X.L. and Y.W.; visualization, X.X. (Xiaohan Xu), A.X., Z.W., Y.S., X.X. (Xuefeng Xu) and Z.Z.; project administration, X.X. (Xiaohan Xu) and Y.W.; funding acquisition, Z.Z., X.L. and Y.W. All authors have read and agreed to the published version of the manuscript.

Funding: This research was funded by Jiangsu Agricultural Industry Technology System (JATS[2023]416), the National Natural Science Foundation of China (31770733, 32202544, 31470490), Key Research and Development Program of Jiangsu (BE2023364), National Key Research and Development Program of China (2022YFD1200505), and the Science and technology projects of Nanjing (202210013).

Data Availability Statement: The original contributions presented in the study are included in the article and Supplementary Materials, further inquiries can be directed to the corresponding author.

Acknowledgments: We thank Yuehua Ma (Central Laboratory of College of Horticulture, Nanjing Agricultural University) for assistance in using Quantitative real-time PCR (Bio-Rad CFX96, USA).

Conflicts of Interest: The authors declare no conflicts of interest.

References

- Mukhopadhyay, M.; Mondal, T.K.; Chand, P.K. Biotechnological advances in tea (*Camellia sinensis* [L.] O. Kuntze): A review. *Plant Cell Rep.* **2016**, *35*, 255–287. [[CrossRef](#)] [[PubMed](#)]
- Weng, H.; Zeng, X.-T.; Li, S.; Kwong, J.S.W.; Liu, T.-Z.; Wang, X.-H. Tea consumption and risk of bladder cancer: A dose-response meta-analysis. *Front. Physiol.* **2017**, *7*, 693. [[CrossRef](#)]
- Görllich, D.; Prehn, S.; Laskey, R.A.; Hartmann, E. Isolation of a protein that is essential for the first step of nuclear protein import. *Cell* **1994**, *79*, 767–778. [[CrossRef](#)] [[PubMed](#)]
- Harreman, M.T.; Hodel, M.R.; Fanara, P.; Hodel, A.E.; Corbett, A.H. The auto-inhibitory function of importin α is essential in vivo. *J. Biol. Chem.* **2002**, *278*, 5854–5863. [[CrossRef](#)]
- Tamura, K.; Hara-Nishimura, I. Functional insights of nucleocytoplasmic transport in plants. *Front. Plant Sci.* **2014**, *5*, 118. [[CrossRef](#)] [[PubMed](#)]
- Portereiko, M.F.; Sandaklie-Nikolova, L.; Lloyd, A.; Dever, C.A.; Otsuga, D.; Drews, G.N. NUCLEAR FUSION DEFECTIVE1 Encodes the *Arabidopsis* RPL21M protein and is required for karyogamy during female gametophyte development and fertilization. *Plant Physiol.* **2006**, *141*, 957–965. [[CrossRef](#)] [[PubMed](#)]
- Wu, J.-J.; Peng, X.-B.; Li, W.-W.; He, R.; Xin, H.-P.; Sun, M.-X. Mitochondrial GCD1 dysfunction reveals reciprocal cell-to-cell signaling during the maturation of *Arabidopsis* female gametes. *Dev. Cell* **2012**, *23*, 1043–1058. [[CrossRef](#)] [[PubMed](#)]
- Lu, C.; Yu, F.; Tian, L.; Huang, X.; Tan, H.; Xie, Z.; Hao, X.; Li, D.; Luan, S.; Chen, L. RPS9M, a mitochondrial ribosomal protein, is essential for central cell maturation and endosperm development in *Arabidopsis*. *Front. Plant Sci.* **2017**, *8*, 2171. [[CrossRef](#)] [[PubMed](#)]
- Xiong, F.; Duan, C.-Y.; Liu, H.-H.; Wu, J.-H.; Zhang, Z.-H.; Li, S.; Zhang, Y. *Arabidopsis* KETCH1 is critical for the nuclear accumulation of ribosomal proteins and gametogenesis. *Plant Cell* **2020**, *32*, 1270–1284. [[CrossRef](#)]
- Liu, H.H.; Xiong, F.; Duan, C.Y.; Wu, Y.N.; Zhang, Y.; Li, S. Importin beta4 mediates nuclear import of grf-interacting factors to control ovule development in *Arabidopsis*. *Plant Physiol.* **2019**, *179*, 1080–1092. [[CrossRef](#)]
- Blanvillain, R.; Boavida, L.C.; McCormick, S.; Ow, D.W. Exportin1 genes are essential for development and function of the gametophytes in *Arabidopsis thaliana*. *Genetics* **2008**, *180*, 1493–1500. [[CrossRef](#)] [[PubMed](#)]
- Wu, S.J.; Wang, L.C.; Yeh, C.H.; Lu, C.A.; Wu, S.J. Isolation and characterization of the *Arabidopsis* heat-intolerant 2 (hit2) mutant reveal the essential role of the nuclear export receptor EXPORTIN1A (XPO1A) in plant heat tolerance. *New Phytol.* **2010**, *186*, 833–842. [[CrossRef](#)]
- Telfer, A.; Poethig, R.S. HASTY: A gene that regulates the timing of shoot maturation in *Arabidopsis thaliana*. *Development* **1998**, *125*, 1889–1898. [[CrossRef](#)] [[PubMed](#)]
- Bollman, K.M.; Aukerman, M.J.; Park, M.-Y.; Hunter, C.; Berardini, T.Z.; Poethig, R.S. HASTY, the *Arabidopsis* ortholog of exportin 5/MSN5, regulates phase change and morphogenesis. *Development* **2003**, *130*, 1493–1504. [[CrossRef](#)]
- Song, Y.; Cui, H.; Shi, Y.; Xue, J.; Ji, C.; Zhang, C.; Yuan, L.; Li, R. Genome-wide identification and functional characterization of the *Camelina sativa* WRKY gene family in response to abiotic stress. *BMC Genom.* **2020**, *21*, 786. [[CrossRef](#)]
- Chen, C.; Chen, H.; Zhang, Y.; Thomas, H.R.; Frank, M.H.; He, Y.; Xia, R. TBtools: An integrative toolkit developed for interactive analyses of big biological data. *Mol. Plant* **2020**, *13*, 1194–1202. [[CrossRef](#)] [[PubMed](#)]
- Xu, X.; Tao, J.; Xing, A.; Wu, Z.; Xu, Y.; Sun, Y.; Zhu, J.; Dai, X.; Wang, Y. Transcriptome analysis reveals the roles of phytohormone signaling in tea plant (*Camellia sinensis* L.) flower development. *BMC Plant Biol.* **2022**, *22*, 471. [[CrossRef](#)]
- Wang, W.; Sheng, X.; Shu, Z.; Li, D.; Pan, J.; Ye, X.; Chang, P.; Li, X.; Wang, Y. Combined cytological and transcriptomic analysis reveals a nitric oxide signaling pathway involved in cold-inhibited *Camellia sinensis* pollen tube growth. *Front. Plant Sci.* **2016**, *7*, 456. [[CrossRef](#)]
- Duan, Y.; Zhu, X.; Shen, J.; Xing, H.; Zou, Z.; Ma, Y.; Wang, Y.; Fang, W. Genome-wide identification, characterization and expression analysis of the amino acid permease gene family in tea plants (*Camellia sinensis*). *Genomics* **2020**, *112*, 2866–2874. [[CrossRef](#)]
- Sparkes, I.A.; Runions, J.; Kearns, A.; Hawes, C. Rapid, transient expression of fluorescent fusion proteins in tobacco plants and generation of stably transformed plants. *Nat. Protoc.* **2006**, *1*, 2019–2025. [[CrossRef](#)]

21. Pante, N.; Kann, M. Nuclear pore complex is able to transport macromolecules with diameters of about 39 nm. *Mol. Biol. Cell* **2002**, *13*, 425–434. [[CrossRef](#)] [[PubMed](#)]
22. Lee, S.J.; Sekimoto, T.; Yamashita, E.; Nagoshi, E.; Nakagawa, A.; Imamoto, N.; Yoshimura, M.; Sakai, H.; Chong, K.T.; Tsukihara, T.; et al. The structure of importin-beta bound to SREBP-2: Nuclear import of a transcription factor. *Science* **2003**, *302*, 1571–1575. [[CrossRef](#)] [[PubMed](#)]
23. Cingolani, G.; Petosa, C.; Weis, K.; Muller, C.W. Structure of importin-beta bound to the IBB domain of importin-alpha. *Nature* **1999**, *399*, 221–229. [[CrossRef](#)] [[PubMed](#)]
24. Chook, Y.M.; Blobel, G. Structure of the nuclear transport complex karyopherin-beta2-Ran x GppNHp. *Nature* **1999**, *399*, 230–237. [[CrossRef](#)] [[PubMed](#)]
25. Bayliss, R.; Littlewood, T.; Stewart, M. Structural basis for the interaction between FxFG nucleoporin repeats and importin-beta in nuclear trafficking. *Cell* **2000**, *102*, 99–108. [[CrossRef](#)] [[PubMed](#)]
26. Xu, G.; Guo, C.; Shan, H.; Kong, H. Divergence of duplicate genes in exon-intron structure. *Proc. Natl. Acad. Sci. USA* **2012**, *109*, 1187–1192. [[CrossRef](#)]
27. Oh, T.R.; Yu, S.G.; Yang, H.W.; Kim, J.H.; Kim, W.T. AtKPNB1, an Arabidopsis importin-beta protein, is downstream of the RING E3 ubiquitin ligase AtAIRP1 in the ABA-mediated drought stress response. *Planta* **2020**, *252*, 93. [[CrossRef](#)]

Disclaimer/Publisher’s Note: The statements, opinions and data contained in all publications are solely those of the individual author(s) and contributor(s) and not of MDPI and/or the editor(s). MDPI and/or the editor(s) disclaim responsibility for any injury to people or property resulting from any ideas, methods, instructions or products referred to in the content.